

Study of the Optical, Structural and Morphological Properties of Electrodeposited Copper Manganese Sulfide (CuMnS) Thin Films for Possible Device Applications

Augustine Nwode Nwori^{1,*}, Laz Nnaedozie Ezenwaka¹, Ifeyinwa Euphemia Ottih¹, Ngozi Agatha Okereke¹ and Nonso Livinus Okoli²

¹Department of Industrial Physics, Faculty of Physical Science, Chukwuemeka Odumegwu Ojukwu University, Uli, Anambra State 431124, Nigeria

²Department of Physics and Electronics, Faculty of Natural and Applied Sciences, Legacy University, Okija, Anambra State 431119, Nigeria

(* Corresponding Author's e-mail: austine2010forreal@yahoo.com)

Received: 3 June 2021, Revised: 26 August 2021, Accepted: 3 September 2021

Abstract

Semiconductor thin films of CuMnS have been deposited onto conductive fluorine-doped tin oxide (FTO) glass substrate using an electrodeposition method to investigate their properties for possible applications. Copper sulfate, manganese sulfate and Thiourea were precursors used for sources of copper, manganese and sulphur ions respectively. The concentration of manganese ions was varied while keeping deposition voltage and time constant at 0.6 and 100 s, respectively. The films were characterized for optical, structural and morphological properties. The results obtained showed that the absorbance of the films is high in the visible (VIS) and near-infrared (NIR) regions but decreases towards NIR. The films transmittance is low in the VIS but increased in the NIR regions. The extinction coefficient is low in the VIS and NIR regions and decreases as concentration of manganese ion increased. The refractive index is high and initially increased slightly from 4.49 to 4.68 in the mid-VIS region while manganese concentration increased from 0.05 to 0.15 M and then decreased to the value of 2.73 as concentration of manganese ion increased further. The optical conductivity is high throughout the VIS and NIR regions while the optical bandgap energy is in the range of 1.5 to 2.05 eV and increases as manganese ion concentration increased. The XRD analysis showed that the deposited thin films of CuMnS are crystalline with average crystallite size and micro-strain in the range of 15.86 - 24.45 nm and 3.97×10^{-3} - 6.13×10^{-3} , respectively. The SEM results showed that the films are composed of particle sizes that are spherical in shape, uniform in sizes and densely packed together and consequently make the film surface rough. These properties exhibited by the films make them good materials for applications in photovoltaic cells, solar control coatings, photothermal applications and many other electronic devices that require high temperatures.

Keywords: Thin films, Electrodeposition, Bandgap, X-ray diffraction, Morphology, Photovoltaic Cell

Introduction

Copper sulphide CuS is one of the important p-type semiconductor materials which have been adjourned to be very useful for copious applications such as in electro-conductive coatings, photo-thermal conversion applications, photovoltaic applications, solar coatings, photodetectors, gas sensors, superconductors, microwave shield coating, promising nanometer-scale switch and many other electronic and optoelectronic device applications, [1-3]. About 5 stable phases of the copper sulphide (Cu_xS : $1 \leq x \leq 2$) systems are known to exist naturally and included the following: Covellite ($\text{Cu}_{1.00}\text{S}$), anilite ($\text{Cu}_{1.7}\text{S}$), digenite ($\text{Cu}_{1.80}\text{S}$), djurleite ($\text{Cu}_{1.97}\text{S}$), and chalcocite ($\text{Cu}_{2.00}\text{S}$) phases, [4,5]. The bandgap energy of CuS thin films is in the range of 1.2 - 2.5 eV and as such mainly useful for photovoltaic applications, [6,7]. The incorporation of foreign materials (dopant ions) into the host semiconductor crystals (in the case of CuS) have been noted to alter its various properties. Of particular interest is the control of the bandgap energy and positions of the Fermi level and most importantly different nanostructures are obtained in most of the semiconductor thin films when incorporated with foreign element, [8-10]. The incorporation

of elements such as iron (Fe), manganese (Mn), nickel (Ni), cobalt (Co) that have self-induced spin electronic properties into chalcogenides semiconductor thin film materials such as CuS have been known to demonstrate high performance potentials for many device applications. The high performance potentials is because sizeable numbers of the ions of such elements (Mn^{2+} , Fe^{2+} , Co^{2+} etc) give rise to varieties of cooperative effects through process of spin-spin exchange interactions, [11,12]. To that effect, [13] used electrodeposition technique to grow CuMnS composites on a Ni-substrate and reported that electrochemical properties of CuMnS electrodes displayed maximum specific capacitances of 2290 F/g at 10 A/g current density and uniform capacitance retention rate (~94 %) after 2500 charging-discharging cycles. Ref [14] used hydrothermal method to fabricate CuS/MnS composite hexagonal nanosheet clusters and reported that the specific capacitance of CuS/MnS composite electrode fabricated is 5 times higher than that of either CuS or MnS electrode when exposed under the same conditions. They went further to conclude that CuS/MnS nano-composite is a promising electrode material for supercapacitors device application. Akunna *et al.* [15] investigated the effect of concentration of manganese ion on the optical properties of manganese alloyed copper (II) sulphide thin films deposited by chemical bath deposition method and inferred that the manganese ion concentration influenced various optical properties such as absorbance, reflectance, refractive index, extinction coefficient, transmittance and bandgap energy of the films and as such can be used for many opto-electronic applications. In this paper, the aim is to investigate the optical, structural and morphological properties of the CuS incorporated with manganese by using electrodeposition technique to fabricate their thin films on FTO glass substrate for possible device applications. The electrodeposition is preferred because of its cost effectiveness and ease of deposition

Materials and methods

Ternary chalcogenide thin films of CuMnS were deposited on fluorine tin oxide (FTO) conductive glass substrate using an electrodeposition method. Copper sulphate ($CuSO_4 \cdot 4H_2O$) (Guangdong Guanghua Sci.-TechCo., Ltd), manganese sulphate ($MnSO_4 \cdot H_2O$) (Guangdong Guanghua Sci.-Tech Co., Ltd) and thiourea (CH_4N_2S) (Guangdong Guanghua Sci.-Tech Co., Ltd) were the main precursors used in the fabrications of the thin film samples. The $MnSO_4 \cdot H_2O$ was used as the sources of manganese ions while $CuSO_4 \cdot H_2O$ and CH_4N_2S served as sources of copper and sulphur ions, respectively. Sodium trisulphate (Na_2SO_3) (Qualikens Laboratory Reagent) and Ethylenediaminetetraacetic acid (EDTA) (Hangzhou Lingui Chemical Co. Ltd) was used to serve as supporting electrolyte and complexing agents respectively. The fluorine-doped tin oxide (FTO) conductive glass substrate (working electrode) before its use as cathode electrode was washed with acetone in an ultrasonic machine for 1 h and dried in an electric oven.

The platinum rod was used as a counter electrode and the surface was thoroughly cleaned for free flow of current. Ag/AgCl electrode was used as reference electrode of known potential. Three electrode system arrangement of electrodeposition was employed to deposit thin films of CuMnS using potentiostat (model Zhaoxin: RXN-3010D) electrodeposition machine set at a constant voltage of 0.6 V. The experimental details and procedures which involved a variation of the concentration of manganese source while keeping other parameters constant are summarized and presented in **Table 1**; A total of 5 samples were produced and are named as 0.05 M, 0.10 M, 0.15 M, 0.20 M and 0.25 M.

Table 1 Preparation of CuMnS thin films at varying concentration of Mn^{2+} source.

Bath Name	$CuSO_4 \cdot 5H_2O$		$MnSO_4 \cdot H_2O$		CH_4N_2S		EDTA		Na_2SO_4		Voltage (Volt)	Time (secs)
	Conc. (Mol)	Vol (mL)	Conc. (Mol)	Vol (mL)	Conc. (Mol)	Vol (mL)	Conc. (Mol)	Vol (mL)	Conc. (Mol)	Vol (mL)		
0.05 M	0.2	0.2	0.05	10	0.1	10	0.025	5.0	0.05	10	0.6	100
0.10 M	0.2	0.2	0.10	10	0.1	10	0.025	5.0	0.05	10	0.6	100
0.15 M	0.2	0.2	0.15	10	0.1	10	0.025	5.0	0.05	10	0.6	100
0.20 M	0.2	0.2	0.20	10	0.1	10	0.025	5.0	0.05	10	0.6	100
0.25 M	0.2	0.2	0.25	10	0.1	10	0.025	5.0	0.05	10	0.6	100

The deposited thin films of CuMnS were annealed at a temperature of 250 °C for 5 min to improve their quality and characterized for the optical properties using 756S UV-VIS Spectrophotometer, structural properties using EMPYREAN Diffractometer and the morphological properties were investigated using MIRA 3 TESCAN scanning electron microscope (SEM).

Results and discussion

Optical analysis

The absorbance of the films was measured from the UV-VIS spectrophotometer machine and the plot of the absorbance of the deposited thin films of CuMnS as a function of wavelength is displayed in **Figure 1**. The figure shows that the absorbance of the films is high in visible (VIS) region but decreases in the near-infrared (NIR) region. It is also observed that the absorbance of the films decreases with an increase in the concentration of manganese (Mn) precursor though there is a discrepancy in the absorbance of the films mostly in the VIS region. The discrepancy can be attributed to the discrepancy in the film thickness. In addition, CuS have been known to exhibit different absorbance edges in the electromagnetic spectrum (UV and VIS regions), [16]. This result is similar to the results of CuMnS thin deposited by the chemical bath method as reported by Salem *et al.* [17].

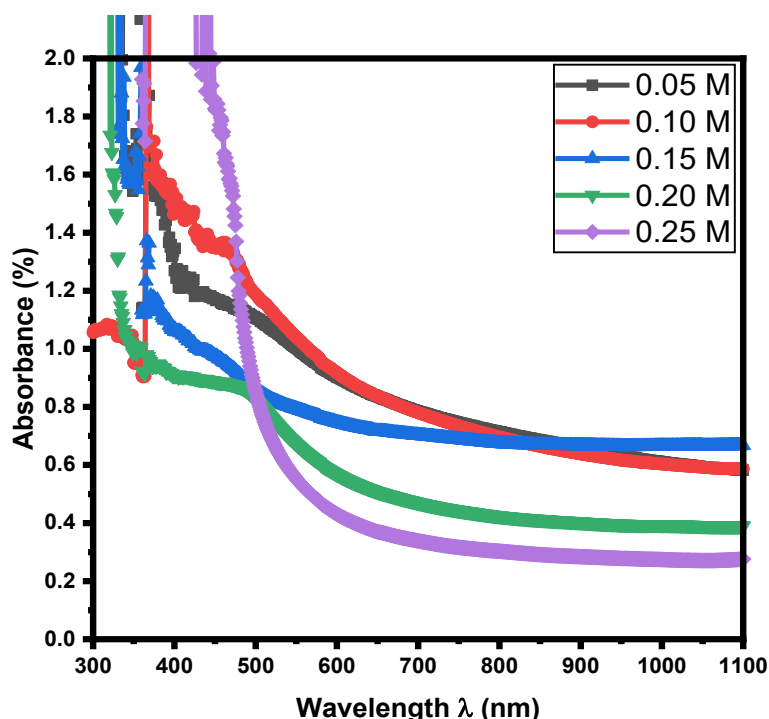


Figure 1 Graph of Absorbance against wavelength for the deposited films.

The transmittance of the films was calculated using the relation given by [18].

$$T = 10^{-A} \quad (1)$$

Where A is the measured absorbance of the films.

Figure 2 is the graph of the percentage transmittance of the films against wavelength. From the figure, it is observed that the transmittance of the films increases with an increase in both wavelength and concentration of Mn source.

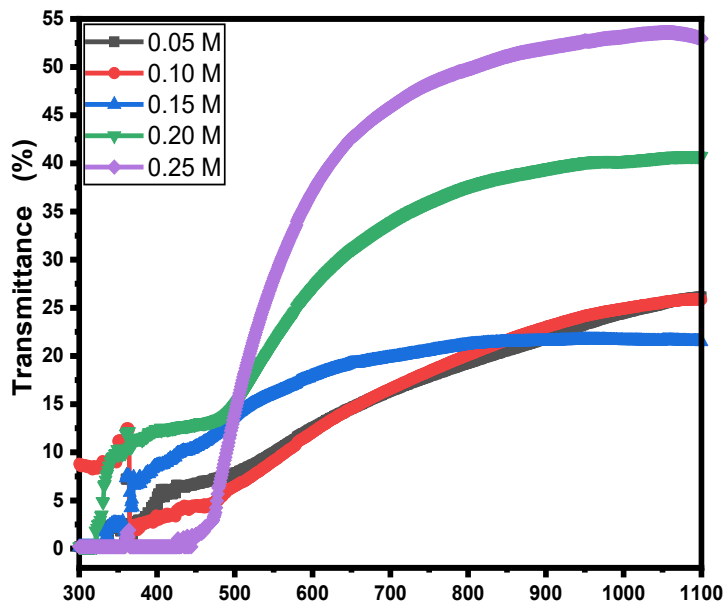


Figure 2 Graph of percentage transmittance against wavelength for the deposited films.

The extinction coefficient of the deposited thin films was calculated using the relation given by [19].

$$K = \frac{\alpha\lambda}{4\pi} \tag{2}$$

The plot of extinction coefficient against wavelength for the deposited thin films of CuMnS is shown in Figure 3. The figure indicates that the extinction coefficient of the films is high throughout the VIS and NIR regions of electromagnetic spectrum. The values of the extinction coefficient of the films also decrease as the concentration of the Mn ion source increased.

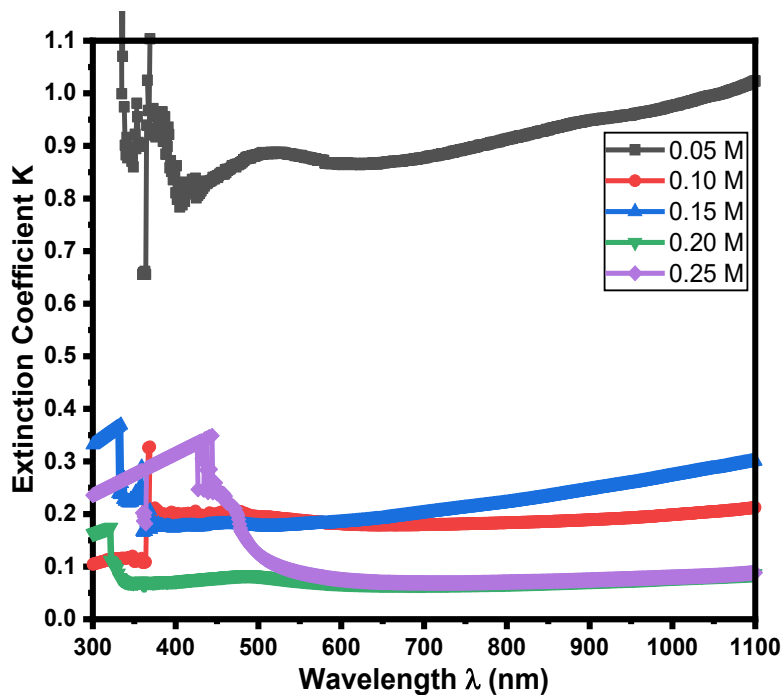


Figure 3 Graph of extinction coefficient against wavelength for the deposited films.

The refractive index of the films was obtained from the relation given by, [20,21].

$$n = \frac{1+R}{1-R} + \sqrt{\frac{4R}{(1-R)^2} - K^2} \quad (3)$$

Where R is the reflectance of the films which was obtained from the relation, [22].

$$T = (1 - R)^2 e^{-A} \quad (4)$$

Figure 4 shows the graph of the refractive index of the films against wavelength. From the figure, it is observed that the refractive index of the films is high both in the VIS and NIR regions but higher in the VIS region. The refractive index is high and initially increased slightly from 4.49 to 4.68 in the mid-VIS region while manganese concentration increased from 0.05 M to 0.15 M and then decreased to the value of 2.73 with further increase in the concentration of manganese ion sources. The range of values of the refractive index of the films is 2.5 - 7.0 in the VIS while in the NIR region its range is 2.5 - 4.25. The high value of the refractive index of the films can be attributed to the high absorption nature of the films. That is, the speed of light in the films can be greatly lowered since the high portion of the light is absorbed. This property makes the films good for waveguide applications.

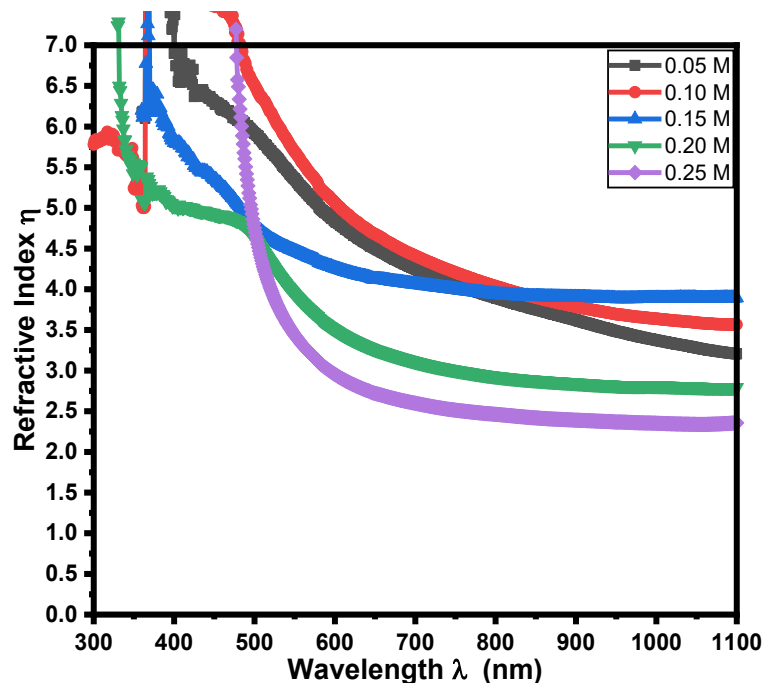


Figure 4 Graph of refractive index against wavelength for the deposited films.

The optical conductivity of the deposited thin films was calculated using the relation given by [23].

$$\sigma = \frac{\alpha \eta C}{4\pi} \quad (5)$$

Where α is the absorption coefficient, η is the refractive index and C is the speed of light. The plot of the optical conductivity of the deposited thin films of CuMnS as a function of wavelength is shown in **Figure 5**. From the figure, it is found that the optical conductivity of the films is generally high throughout the VIS and NIR regions but are lower in the NIR region. The value of the optical conductivity of the films however decreases as the concentration of Mn ion precursor increased in both VIS and NIR regions.

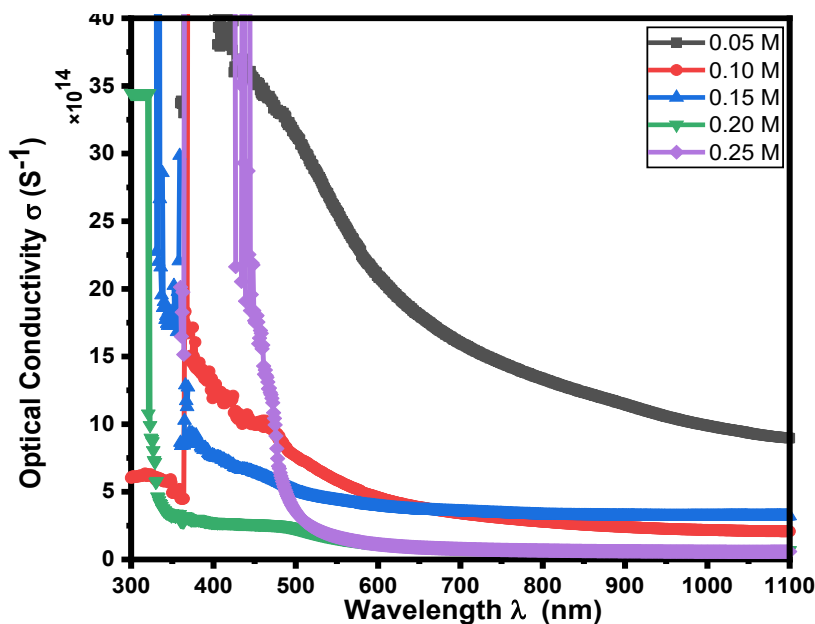


Figure 5 Graph of optical conductivity against wavelength for the deposited films.

The bandgap energy of the deposited thin films of CuMnS was calculated using the Tauc's relation given by [24,25].

$$(\alpha h\nu) = A(h\nu - E_g)^n \quad (6)$$

Where α is the absorption coefficient of the films, $h\nu$ is the photon energy, A is a constant factor, E_g is the energy bandgap and "n" is the transition type factor; which gives direct allowed transition for n equals to $\frac{1}{2}$ and indirect allowed transition for n equals to 2. The absorption coefficient (α) used in Eqs. (5) and (6) was calculated using the relation given as [26].

$$\alpha = \frac{1}{t_f} \ln \left[\frac{(1-R)^2}{T} \right] \quad (7)$$

Where T , R and t_f are the transmittance, reflectance and thickness of the films respectively. The thickness of the films was obtained by the weight gain method according to the relation as given by [27,28].

$$t_f = \frac{M}{\rho S_a} \quad (8)$$

Where M represents the mass of the thin films deposited on the surface of the FTO glass substrate, which was calculated via the equation.

$$M = m_2 - m_1 \quad (9)$$

Where m_1 is the mass of plain FTO glass before film deposition, m_2 is the mass weighted by the FTO glass after film deposition, ρ is the average of the bulk densities (g/cm^3) of CuS and Mn, while S_a is the surface area of the thin films on the substrate. The values of the thickness of the films calculated via this method were 50.45, 245.35, 197.17, 401.66 and 277.30 nm for the 0.05, 0.15, 0.20 and 0.25 M films, respectively.

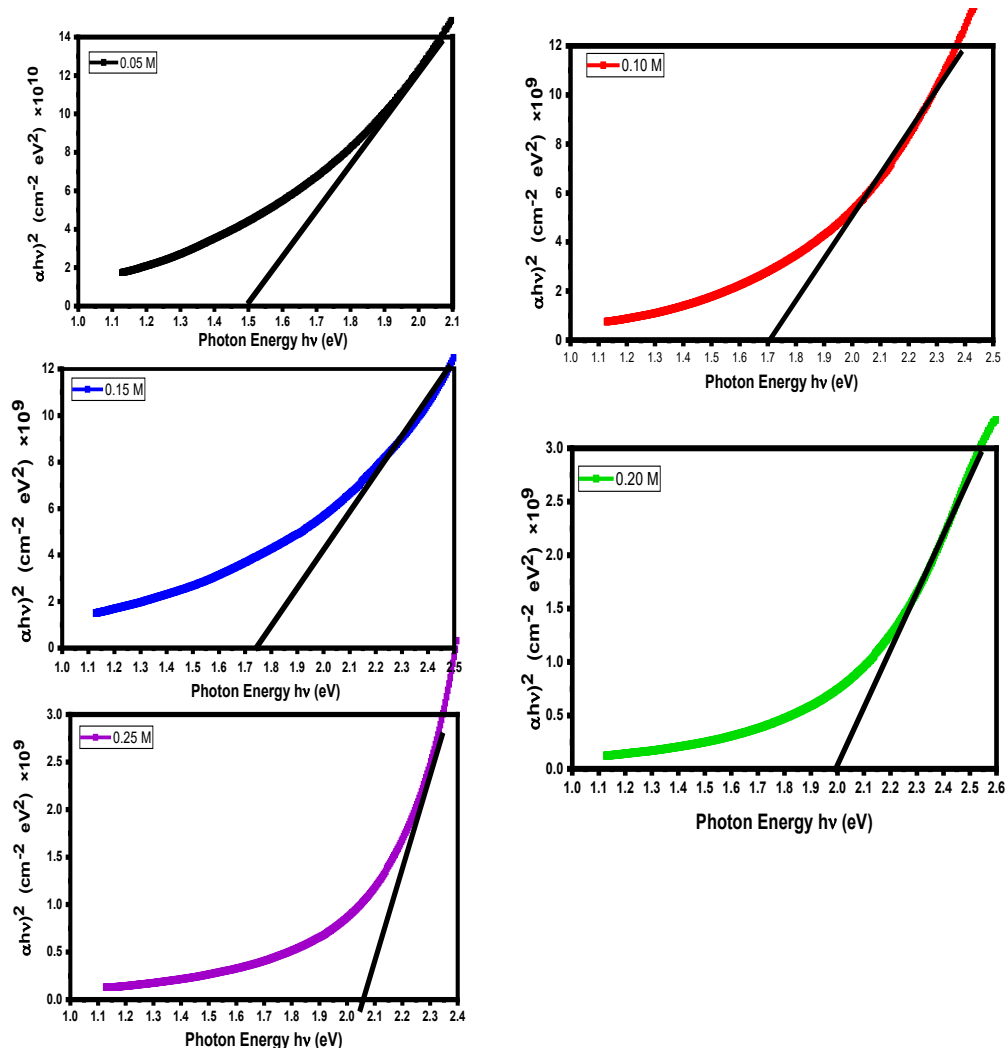


Figure 6 Plots of $(\alpha hv)^2$ against photon energy (hv) for the deposited films.

The plot of $(\alpha hv)^2$ against photon energy (hv) for determination of the optical bandgap energy of the films are displayed in **Figure 6**. From the figure, the bandgap energy of the deposited thin films was obtained by extrapolating the curves of the plots for the samples along the energy axis (photon hv). The bandgap energy of the films was found to increase as concentration of Mn ion increased. The values of the bandgap energy of the deposited thin films can be seen to be 1.5, 1.7, 1.75, 2.0 and 2.05 eV for the films 0.05 M, 0.10 M, 0.15 M, 0.20 M and 0.25 M, respectively. These values of bandgap are in the solar spectrum range; therefore, the films are suitable for photovoltaic cell application for conversion of solar energy to electricity.

Structural properties

The results of the XRD analysis done to determine the structural properties of the deposited thin films of CuMnS is displayed in **Figure 7**. From the figure, it is observed from the XRD patterns of the films that the films are crystalline as there are sharp peaks that occurred at 2 theta positions 26.150, 33.370, 37.410, 51.190, 61.240, and 65.210 degrees. These 2 theta positions are indexed to crystalline planes of (2110), (222), (302), (422), (442) and (343), respectively. These peaks match pretty well with the standard data (JCPDS Nos. 00-050-0540 and 00-033-0489) indexed to the cubic crystal structure of Cu_2MnS_2 and orthorhombic structure of the anilite-phase Cu_7S_4 of copper sulfide. The average crystallite size (D), dislocation density (δ) and micro-strain (ϵ) of the films were calculated using the Dybe-Scherer and Williamson-Smallman relation given by [29-31].

$$D = \frac{k\lambda}{\beta \cos\theta} \quad (10)$$

$$\delta = \frac{1}{D^2} \quad (11)$$

$$\varepsilon = \frac{\beta}{4 \tan\theta} \quad (12)$$

Where k is the shape factor, λ is the X-ray wavelength, β is the full width at half maximum (FWHM) and θ is the Bragg's angle. The average crystallite size (D), dislocation density (δ) and micro-strain (ε) of the films calculated are presented in **Table 2**.

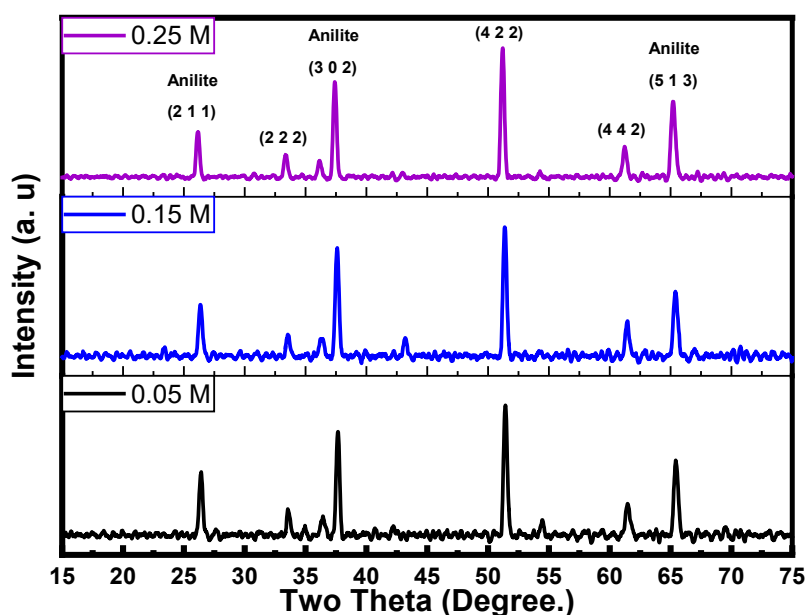


Figure 7 XRD patterns of the deposited thin films of CuMnS.

Table 2 Average crystallite size, dislocation density and micro-strain of CuMnS thin films.

Samples	Crystallite Size D (nm)	Dislocation Density δ (lines/nm ²)	Micro-strain (ε)
0.25 M	15.86	3.97×10^{-3}	6.13×10^{-3}
0.15 M	23.70	1.78×10^{-3}	4.20×10^{-3}
0.05 M	24.45	1.67×10^{-3}	3.97×10^{-3}

Morphological properties

Figure 8 is the scanning electron microscope (SEM) morphology of the deposited thin films of CuMnS. In the figure, it can be seen from the SEM morphology that the particle sizes of the films are uniformly packed together on the surface of the conductive FTO glass substrate. The particle sizes are spherical in shape, uniform in size and densely packed together thus revealing the rough nature of the surface of the films. The morphology of the films further indicates that there are no pores or hollows on the surface of most of the films thus confirming the crystalline nature of the deposited thin films.

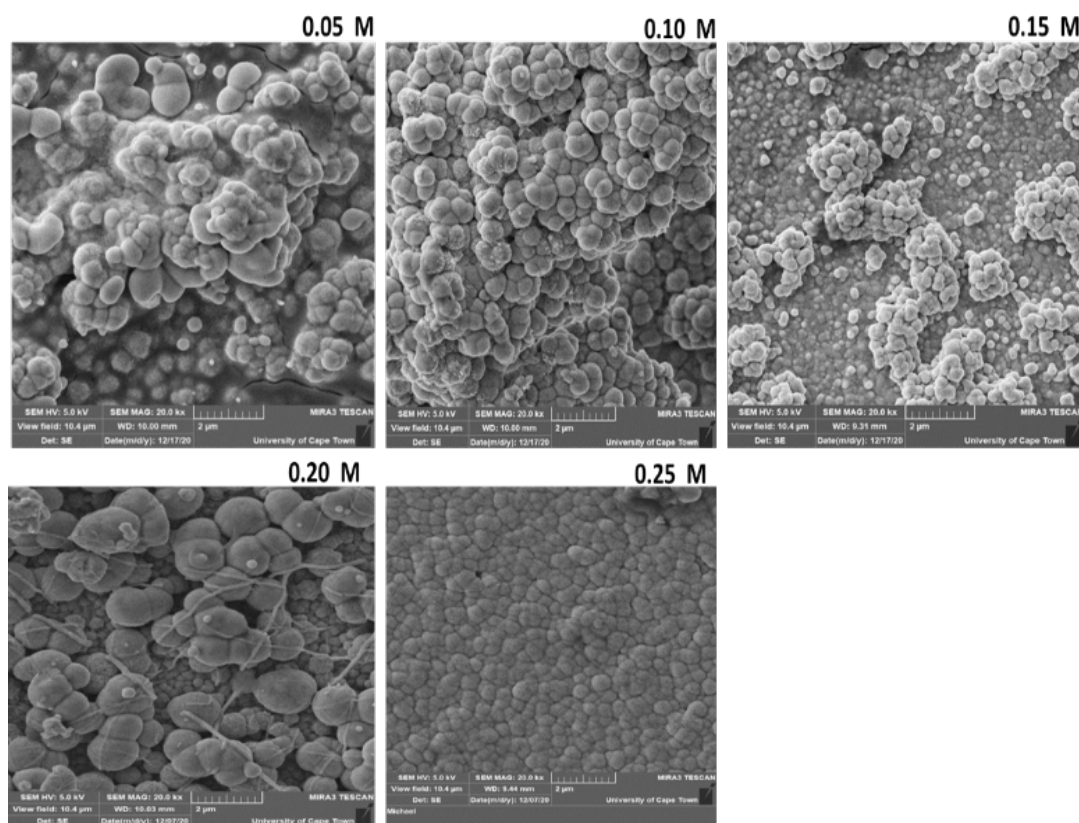


Figure 8 SEM micrographs of the deposited thin films of CuMnS.

Conclusions

The results of the characterization of the deposited ternary chalcogenide thin films of CuMnS showed that the optical absorbance and the optical conductivity of the films are generally high throughout the VIS and NIR regions of the electromagnetic spectrum. The refractive index of the thin films is also found to be high and initially increased slightly from 4.49 to 4.68 in the mid-VIS region as manganese concentration increased from 0.05 M to 0.15 M and thereafter decreased to the value of 2.73 as concentration of manganese ion sources increased further. The extinction coefficient is found to be low and decreased as the concentration of Mn^{2+} increased. The films exhibit wide bandgap energy values which range from 1.5 to 2.05 eV and increased with an increase in Mn^{2+} concentration. The XRD analysis showed that the deposited thin films of CuMnS are crystalline as there exist sharp peaks in the XRD pattern and have cubic and orthorhombic crystal structures. The average crystallite sizes of the films calculated are in the range of 15.86 to 24.66 nm. The SEM micrographs of the films showed that the particle sizes are spherical and are densely packed together thereby revealing the crystalline nature of the films. These properties observed indicate that the films can serve as good materials for photovoltaic cell development, solar control coatings and photothermal applications. The films can also be applied in many other optoelectronic devices that require high temperatures based on the wide-bandgap energy values exhibited by the deposited thin films.

Acknowledgements

We are pleased to appreciate and acknowledge Mr. Whyte F. M., Mr. Nsude Kingsley Ugonna, and Mrs. Nsude Ebere of Nanotech Laboratory, University of Nigeria Nsukka (UNN), Nigeria for their help in carrying out optical characterization, Nura Adamu Mohammed of National Geosciences Research Laboratory, Nigeria Geological Survey Agency, Kaduna State Nigeria for helping in carrying out XRD analysis and Mrs. Miranda Waldron with her team of scientists at Electron Microscope Unit, University of Cape Town South Africa for making their laboratory available to carry out SEM characterization on our samples.

References

- [1] MC Ohakwere-Eze. The growth and characterization of copper sulphide thin films using CBD (chemical bath deposition) technique. *J. Mater. Sci. Eng. B.* 2015; **5**, 181-6.
- [2] MS Shinde, PB Abirao, IJ Patil and RS Patil. Thickness dependent electrical and optical properties of nanocrystalline copper sulphide thin films grown by simple chemical route. *Indian J. Pure Appl. Phys.* 2012; **50**, 657-60.
- [3] YE Firat, H Yildirim, K Erturk and A Peksov. Ultrasonic spray pyrolysis deposited copper sulphide thin films for solar cell applications. *Hindawi Scanning* 2017; **2017**, 2625132.
- [4] HM Pathan and CD Lokhande. Deposition of metal chalcogenide thin films by successive ionic layer adsorption and reaction (SILAR) method. *Bulletin Mater. Sci.* 2004; **27**, 85-111.
- [5] ADA Buba and JSA Adelabu. Electrical conductivity of Cu_xS thin film deposited by chemical bath deposition (CBD) technique. *Nigerian J. Basic Appl. Sci.* 2009; **17**, 161-5.
- [6] NP Huse, DS Upadhyea, AS Dive and R Sharma. Study of opto-electronic properties of copper sulphide thin film grown by chemical bath deposition technique for electronic device application. *Invertis J. Renew. Energy.* 2016; **6**, 74-8.
- [7] E Güneri and A Kariper. Optical properties of amorphous CuS thin films deposited chemically at different pH values. *J. Alloys Compd.* 2012; **516**, 20-6.
- [8] PC Okafor and AJ Ekpunobi. The effect of manganese percentage doping on the thickness and conductivity of copper sulphide nano films prepared by electrodeposition method. *Int. J. Sci Eng. Res.* 2016; **7**, 174-7.
- [9] S Jahan, MNH Liton, MKR Khan and MM Rahman. Effect of aluminum doping on the properties of spray deposited copper sulphide (Cu₂S) thin films. *Int. J. Adv. Eng. Technol.* 2015; **VI**, 23-7.
- [10] P Priyadarshini and R Revathy. Synthesis and characterization of metal doped nano crystalline copper sulphide. *Int. J. Recent Sci. Res.* 2015; **6**, 3328-31.
- [11] PC Okafor and AJ Ekpunobi. Effect of manganese doping percentage on band gap energy of cadmium sulphide (CdS) nano-films prepared by electrodeposition method. *Int. J. Sci. Res.* 2015; **4**, 2280-4.
- [12] N Arbi, IB Assaker, M Gannouni, A Krisa and R Chtourou, Effect of manganese concentration on physical and electrochemical properties of Mn²⁺ doped ZnS thin films deposited onto ITO (glass) substrates by electrodeposition technique. *J. Mater. Sci.: Mater. Electron.* 2017; **28**, 4997-5005.
- [13] MZ Igbal, S Zakar, SS Haider, AM Afzal, MJ Igbal, MA Kamran and A Numan. Electrodeposited CuMnS and CoMnS electrodes for high-performance asymmetric supercapacitor devices. *Ceram. Int.* 2020; **46**, 21343-50.
- [14] H Liu, Z Guo, X Wang, J Hao and J Lian. CuS/MnS composite hexagonal nanosheet clusters: Synthesis and enhanced pseudocapacitive properties. *Electrochim. Acta.* 2018; **271**, 425-32.
- [15] JCC Akunna, LN Ezenwaka, IE Otti and NS Umeokwonna. The effects of concentration on the optical properties of manganese alloyed copper (ii) sulphide thin films deposited by chemical bath deposition technique. *COOU J. Phys. Sci.* 2020; **3**, 362-71.
- [16] KA Mohammed, SM Ahmed and RY Mohammed. Investigation of structure, optical, and electrical properties of CuS thin films by CBD technique. *Crystals* 2020; **10**, 684.
- [17] SM Salem, NM Deraz and HA Saleh. Fabrication and characterization of chemically deposited copper manganese sulfide thin films. *Appl. Phys. A: Mater. Sci. Process.* 2020; **126**, 700.
- [18] IL Ikhioya, PN Okanigbuan, CB Agbakwuru and BU Osolobri. Characterization of zinc sulphide/cadmium sulphide (ZnS/CdS) superlattice by electrodeposition technique. *J. Nigerian Assoc. Math. Phys.* 2015; **29**, 331-8.
- [19] IL Ikhioya, S Ehika and NN Omehe. Electrochemical deposition of lead sulphide (PbS) thin films deposition on zinc plate substrate. *J. Mater. Sci. Res. Rev.* 2018; **1**, 1-11.
- [20] IA Karipers. Optical and structural properties of Bi/Ag-I thin films by co-precipitation method. *Asian J. Chem.* 2016; **28**, 2241-5.
- [21] AA Kadhim, RA Alansary and SA Alhady. Effect of Mn concentration on the structural and optical properties of SnO₂ thin films prepared by pulse laser deposition. *J. Res. Method Educ.* 2014; **4**, 12-9.
- [22] IA Kariper, Ş Özden and FM Tezel. Optical properties of selenium sulfide thin films produced via chemical dropping method. *Opt. Quantum Electron.* 2018; **50**, 144.
- [23] A Ohwofosirai, MD Femi, NA Ngozika, TO Joseph, RU Osuji and BA Ezekoye. A study of the optical conductivity, extinction coefficient and dielectric function of CdO by successive ionic layer adsorption and reaction (SILAR) technique. *Chem. Sci. Int. J.* 201; **4**, 736-44.

- [24] MA Sangamesha, K Pushpalatha, GL Shekar and S Shamsundar. Preparation and characterization of nanocrystalline CuS thin films for dye-sensitized solar cells. *Int. Scholarly Res. Notices*. 2013; **2013**, 829430.
- [25] A Ekpeko and IR Ufuoma. Characterization of copper sulfide (CuS) thin films synthesized by electroless plating. *Int. Res. J. Pure Appl. Phys.* 2019; **6**, 20-35.
- [26] İA Kariper and F Göde. Influence of pH on the structural and optical properties of polycrystalline MnTe₂ thin films produced by chemical bath deposition method. *Acta Phys. Pol. A*. 2017; **132**, 531-4.
- [27] A Hannachi, S Hammami, N Raouafi and H Maghraoui-Meherzi. Preparation of manganese sulfide (MnS) thin films by chemical bath deposition: Application of the experimental design methodology. *J. Alloys Compd.* 2016; **663**, 507-15.
- [28] M Karunakaran, S Maheswari, K Kasirajan, SD Raj and R Chandramohan. Structural and optical properties of Mn-doped ZnO thin films prepared by SILAR Method. *Int. Lett. Chem. Phys. Astron.* 2017; **73**, 22-30.
- [29] M Karunakaran, S Maheswari, K Kasirajan, SD Raj and R Chandramohan. Structural and optical properties of Mn-Doped ZnO thin films prepared by SILAR method. *Int. Lett. Chem. Phys. Astronomy*. 2017; **73**, 22-30.
- [30] AI Hassan and SI Maki. Structural and optical properties of copper-doped cobalt oxide thin films prepared by spray pyrolysis. *Int. J. Eng. Res. Technol.* 2017; **6**, 535.
- [31] K Girija, S Thirumalairajan, SM Mohan and J Chandrasekaran. Structural, morphological and optical studies of CdSe thin films from ammonia bath. *Chalcogenide Lett.* 2009; **6**, 351-7.
- [32] P Prasoon, P Jayaram, NK Sulfikkarali and NK Deepak. Micro-strain, dislocation density, surface morphology and optoelectronic properties of indium zinc oxide thin films. *Int. J. Res. Advent Technol.* 2018; **6**, 3486-91.